

Generation of Ironized and Multivitamin-loaded Liposomes Using Venturi-based Rapid Expansion of Supercritical Solution (Vent-RESS)

Farrokh Sharifi¹, Apratim Jash¹, Alireza Abbaspourrad¹, Syed S.H. Rizvi^{1, 2,*}

¹ Department of Food Science, Cornell University, Ithaca, NY 14850, USA

² School of Chemical and Biomolecular Engineering, Cornell University, Ithaca, NY 14850, USA

*: Corresponding Author, E-mail: srizvi@cornell.edu

Abstract:

Ironized multivitamin-loaded liposomes were generated via supercritical-CO₂ (SC-CO₂) as a green solvent without using any organic solvent. A newly developed, venturi-based rapid expansion of supercritical solution (Vent-RESS) system was employed to bring lipophilic and hydrophilic bioactives in an eductor vacuum system and efficiently mix them together in a fraction of second without the aid of an external pump to generate liposomes. Firstly, two different coating materials, lecithin with 39% and 13% of phosphatidylcholine (PC), were used to study the structure of the resulting liposomes and zeta-potential of the colloidal system. Then, the lecithin with 13% of PC was selected for the microencapsulation purpose due to its better interaction with other hydrophobic components incorporated into the lamellar part of the liposomes. The lipophilic part included the lecithin, cholesterol, and a lipophilic cargo, vitamin E; whereas the hydrophilic phase consisted of iron sulfate and vitamin C solution. It was found that liposomes of unimodal size distribution with an average size range of 580-700 nm were

formed when the SC-CO₂ pressure was changed from 12 to 18 MPa. Additionally, the encapsulation efficiency of vitamins C, E, and iron sulfate were improved to the maximum values of 60%, 88%, and 58% from 46%, 36%, and 12%, respectively when the pressure was increased from 12 to 18 MPa. Finite volume method (FVM) was used to numerically simulate the mixing of the two fluid streams to better understand the effect of hydrophilic cargo introduction geometry on the mixing effectiveness. This microencapsulation system is based on a green approach to generate hydrophilic/lipophilic bioactive-loaded liposomes, free of organic solvents with high potential for scale-up, which can be used in food, biomedical, and cosmetic applications.

1. Introduction:

Liposomes are spherical colloidal vesicles with one or more phospholipid bilayers encapsulating an aqueous phase with different structures: unilamellar vesicles (ULV), multilamellar vesicles (MLV), and multivesicular vesicles (MVV).¹ Owing to their amphiphilic nature, liposomes can microencapsulate both lipophilic and hydrophilic bioactive molecules.^{2, 3} This has drawn much attention from a wide range of applications such as food fortification, drug delivery, and cosmetic preparations.⁴⁻⁷ By surface chemistry modifications, the release of the cargo from the liposomes can be stimulated by pH, light, temperature, and other chemical agents.⁸⁻¹⁰ The properties of the phospholipid bilayer, in terms of permeability and rigidity, can be altered by using different lipid compositions, surfactants, and carbohydrates¹¹⁻¹³ as well as coating with oppositely charged compounds.¹⁴ In food applications, liposomes are used to encapsulate antioxidants, nutrients, enzymes, and other value-added additives.^{6, 15, 16}

Conventional liposome fabrication methods such as thin film hydration (TFH) or the Bangham method and the reverse phase evaporation vesicles (REV) strategy rely on the use of organic solvents such as chloroform and methanol¹⁷; the acute toxicity of the said solvents limits their applications. In order to reduce or stop using organic solvents, supercritical carbon dioxide (SC-CO₂) is used as a green, benign solvent with no toxicity.^{1, 18, 19} In general, supercritical fluids (SCFs) have liquid-like density and gas-like diffusivity, which enable them to dissolve a broad range of compounds, and they have high mass transfer rates.²⁰ Temperature and pressure are the two key factors that control the solubility of different solutes into SCFs. Among all of the SCFs, SC-CO₂ is more common to use due to the fact that it is non-toxic, non-flammable, and inexpensive, with mild critical parameters (critical temperature (T_c)= 31.1 °C and critical pressure (P_c)= 7.39 MPa), which make it possible to work under mild conditions.

In order to reduce or avoid using organic solvents, several relatively new techniques have been applied to produce liposomes, such as the rapid expansion of supercritical solution (RESS), supercritical reverse phase evaporation (scRPE), and expanded solution into aqueous media (DESAM).¹ Among them, RESS and scRPE are the two main strategies, which are used for liposomal microencapsulation.^{21, 22} In the scRPE approach, use of an organic solvent is required to dissolve the phospholipid. Then, liposomes were formed by replacing the organic solvent with SC-CO₂.^{19, 21, 23} In RESS, on the other hand, the coating material is dissolved in SC-CO₂. Then, the supercritical solution passes through a nozzle and a rapid pressure drop occurs, which results in transition of the solvent from a supercritical to a gaseous state. This in turn leads to a

drastic reduction of the coating material solubility in CO₂, and to rapid nucleation of the coating material.²²

Previously, we reported the rapid expansion of the supercritical solution coupled with a venturi system (Vent-RESS) for concomitant vacuum driven cargo loading, based on the Bernoulli principle, to produce glucose-loaded liposomes and studied the effect of operating and geometric parameters on the encapsulation efficiency of the cargo into the liposomes.²² Here, we modified the system to produce ironized multivitamin-loaded liposomes, which include three micronutrients: iron sulfate, vitamin C, and vitamin E. The hydrophilic cargo (iron sulfate and vitamin C) were encapsulated into the aqueous core, whereas the lipophilic cargo (vitamin E) was entrapped inside the phospholipid coating material. The modifications were conducted in the coating material and post-processing parts. The liposomes were analyzed in terms of type, structure, size, surface charge, and encapsulation efficiency of the cargo in the liposomes. In addition to the experimental work, the mixing of two fluids, i.e. CO₂ and hydrophilic cargo solution, was simulated using finite volume method (FVM). The numerical work illustrated the impact of the hydrophilic cargo introduction stream on the mixing effectiveness: flow trajectories, streamlines, and velocity distributions of the fluids within the educator-nozzle system.

2. Materials and Method

2.1 Materials

Tris(hydroxymethyl) aminomethane (TRIS) was obtained from Bio-Rad (Hercules, CA, USA). Nile Red, fluorescein isothiocyanate (FITC), cholesterol (95% minimum purity), vitamin E, dimethyl sulfoxide (DMSO), and protamine sulfate were purchased from

Sigma-Aldrich (St. Louis, MO, USA). Iron sulfate heptahydrate was obtained from Honeywell (Charlotte, NC, USA). L-ascorbic acid (i.e. vitamin C) was purchased from TCI America (Portland, OR, USA). Carbon dioxide (CO₂) (minimum purity 99.99%) was purchased from Airgas (Ithaca, NY, USA). The coating material of the liposomes was made by using two types of lecithin: i. SOLEC FP 40 with 39% of phosphatidylcholine (PC), 20% phosphatidylethanolamine (PE), and 3% phosphatidylinositol (PI), which was provided by DuPont (New Century, KS, USA). ii. Performix™E soy lecithin, containing 13% phosphatidylcholine (PC), 11% phosphatidylethanolamine (PE), and 8% phosphatidylinositol (PI), and was provided by Archer Daniels Midland Company (Chicago, IL, USA).

2.2. Preparation of the aqueous cargo solution and carrier

Aqueous cargo solution: 0.8 M iron sulfate heptahydrate and 0.125 M ascorbic acid (vitamin C) were dissolved in a 0.02 M TRIS buffer solution with the pH of 7.4.

Lipophilic cargo and carrier: Lecithin, cholesterol, and vitamin E, were combined with a weight (gram) ratio of 10:1:1 and were thoroughly mixed until a homogeneous mixture was obtained, and then the mixture was transferred to the vessel for dissolving in SC-CO₂. Cholesterol was used because it interacts with the hydrophilic/hydrophobic ends of the phospholipid bilayer, restrict the movements of acyl chains in the phospholipid bilayer, and thus provides additional rigidity to the liposomal membrane and enhance Young's modulus of liposomes, which helps to prevent their structural disintegration.^{2, 24, 25} The mixture was stored at 4 °C to be solidified for loading convenience. The weights of the three components used in the vessel was more than the solubility of SC-CO₂ at all of

our operating conditions (60 °C and 12-18 MPa) ^{2, 22, 26} to make sure that the SC-CO₂ would be saturated with the three components after getting to the equilibrium condition. This work helped to keep the system in the equilibrium condition and generate liposomes multiple times.

2.3 Method: Liposome production using a SC-CO₂ platform

Figure 1 shows the schematic of the Vent-RESS system, which was used to generate liposomes. In order to ensure CO₂ was in liquid state before feeding into a high-pressure liquid pump, a heat exchanger was used, then it was preheated, and transferred to a high-pressure mixing-vessel with a set temperature of 60°C (**Figure 1 (a)**). The mixing-vessel was preloaded with the lipophilic cargo (vitamin E) and the carrier (lecithin and cholesterol). Inside the mixing-vessel the lipophilic cargo and the carrier mixture was mixed with SC-CO₂ under continuous stirring for one hour to obtain equilibrium. Within this time, the lipophilic cargo and the phospholipids in lecithin were dissolved in SC-CO₂. The next step was to transfer the coating/cargo-laden (CCL) SC-CO₂ to the nozzle part. To avoid precipitation before entering the nozzle, the temperature of the SC-CO₂ was kept constant at 60 °C. Then, the high-pressure CCL SC-CO₂ passed through the nozzle and its velocity significantly increased at the *vena contracta* and its pressure dropped to below atmospheric pressure (Bernoulli's principle), this resulted in the creation of vacuum, which facilitated the suction of the hydrophilic cargo solution into the educator-nozzle assembly (**Figure 1 (b)**). A 1.5 mm converging nozzle was positioned in the educator in a way that its distance from the cargo introduction tube (I.D. 1.3 mm) was 5 cm. Inside the educator, post-expansion, SC-CO₂ loses its supercritical properties, and this results in super-

saturation of both the coating material and the lipophilic cargo in CO₂, thereby causing their atomized nucleation. The pulled-in hydrophilic cargo stream gets fractionated into microscopic droplets because of the high shear force exerted by the released downstream-CO₂ and the nucleated lipophilic material. Adequate mixing between the hydrophilic cargo and the cargo-laden lipophilic material allows the coating of hydrophilic cargo droplets with phospholipid bilayers, and thus liposomes were formed (**Figure 1 (b)**).² Since the Joule-Thompson effect might negatively impact the process by creating a large temperature drop, the eductor nozzle was held at 80°C, which is above the phase transition temperature of lecithin (40-42 °C). This also reduces the interfacial tension between the vitamin E-laden phospholipids and the hydrophilic cargo to increase their mixing.^{2, 27-29} The liposome production process was done at three different SC-CO₂ expansion pressures of 12, 15, and 18 MPa to better understand the effect of SC-CO₂ expansion pressures. The experimental details are summarized in **Table 1**.

2.4 Separation of coated and uncoated iron sulfate

The rapid oxidation of ferrous oxide is a factor that needs to be considered to obtain stable colloidal system. To obtain stable liposomal dispersion, following procedure was pursued: i. Ascorbic acid was used in both cargo and collecting buffer solutions (Ascorbic acid: Iron sulfate weight ratio was 1:10). Ascorbic acid inhibits ferrous oxidation owing to its chelating and reducing properties; ii. Cationic exchange resins, which are negatively charged were used with the concentration of 0.1 g/mL in the collecting buffer to absorb the uncoated (free) Iron and separate them from the coated iron sulfate (**Figure 1 (c)**); and iii. A cargo introduction pipe with a diameter of 2 mm (ID) was used to reduce the

cargo flow rate and limit the exposure of the cargo to oxygen before mixing with the coating material. It was observed that if the unencapsulated ferrous sulfate molecules were not separated from the encapsulated ones, their oxidation leads to liposome rupture (**Figure 2(a)**). By doing the steps i-iii, highly stable liposomes were created that lasted for weeks in the buffer without rupture (**Figure 2(b)**).

2.5 Morphology

Confocal laser scanning microscopy (CLSM) was used to study the morphology of the synthesized liposomes. Images were taken by using a Zeiss LSM 710 confocal microscope equipped with 63x oil-phase objective lens. For better visualization purpose, synthesized liposomes were stained by the method described by Tsai and Rizvi². Briefly, FITC and Nile red were used to stain the hydrophilic core and the lipophilic bilayer parts, respectively. The fluorescence emission spectrum of FITC and Nile Red was set between 496-535 nm and 558-635 nm, respectively. 5 mM FITC was prepared in TRIS buffer at pH 7.4 and it was used as the hydrophilic cargo solution. After making the liposomes, the phospholipid bilayer was stained with Nile red. For this part, 0.2 wt% Nile Red was dissolved in ethanol. Then, 10 μ L of Nile Red solution was added to 1 mL of FITC loaded liposomes and mildly agitated by hand for 1 min. Then, the stained liposome suspension was used for confocal laser scanning microscopy (CLSM). Additionally, in order to study the structure and morphology of the liposomes made using two different coating materials, scanning electron microscopy (SEM; JCM-6000 NeoScope Benchtop scanning electron microscope) was applied. Glycerol with the concentration of 10% (V:V) was used as a stabilizing excipient to dehydrate the liposomes without affecting the size or cargo

encapsulation efficiency.³⁰ For drying, 50 μ L of the liposome suspension was pipetted onto a SEM stub. Then, the sample was rapidly frozen using liquid Nitrogen at -195.79 °C, followed by rapid transfer into a freeze dryer, where it was incubated for 24 hours. At the end, the samples were coated with gold using sputter coating to make the sample conductive for SEM imaging.

2.6 Size analysis and zeta potential

90 PLUS particle size analyzer (Brookhaven Instruments Corporation, Holtsville, NY, USA) equipped with BI-zeta extension was used to obtain the size distribution and zeta potential of the liposomes made with different conditions and coating formula. For the measurement, the liposome suspension was diluted 10 times with TRIS buffer to avoid reducing the scattered light that is being detected by the instrument.

2.7 Encapsulation efficiency

The encapsulation efficiency (EE) of the aqueous cargo (vitamins C) was determined using the protamine aggregation method.³¹ Briefly, 0.1 ml of the liposomal emulsion was mixed with protamine solution (10 mg/mL) with the volume ratio of 1:1 and was left for 3 minutes. Then, it was mixed with 1.3 mL of a 0.9% w/v saline solution, followed by centrifugation 2000xg for 25 min at 4 °C. After removing the supernatant from the sample, 0.6 mL of a 10% w/v Triton X-100 solution was added into the concentrated and purified samples and the sample was agitated using a vortex for 5 minutes to rupture the liposomes. Then, saline solution was added to the mixture to give it a final volume of 3 mL. UV/Vis Spectrophotometry (UV/Vis Spectrophotometer UV1900, Shimadzu

Scientific Instruments/Marlborough, MA, USA) was used to measure the absorbance values of vitamin C at the wavelength of 265 nm.

For vitamin E a new protocol was developed to measure the encapsulation efficiency. 1.5 ml liposomal dispersion was centrifuged at 1500xg for 20 minutes. The supernatant was separated out and 0.2 ml DMSO was separately added to both concentrated liposome and supernatant, followed by dilution with TRIS buffer. DMSO was used as it can dissolve both vitamin E and PC. UV/Vis Spectrophotometry was used to measure the absorbance values of vitamin E at the wavelength of 295 nm. Then, the encapsulation efficiency of each cargo was calculated using the equation below ³²:

$$\text{EE for vitamin C and E (\%)} = \frac{\text{vitamin content in centrifuged liposomes}}{(\text{vitamin content in centrifuged liposomes} + \text{vitamin content in supernatant})} \times 100 \quad [1]$$

Additionally, Inductively Coupled Plasma Atomic Emission Spectroscopy (ICP-AES) was used to measure the ferrous iron content in liposomes. The encapsulation efficiency of ferrous iron was calculated using equation 2:

$$\text{EE for iron (\%)} = \frac{\text{Iron content in liposomes}}{\text{Total iron content in cargo solution}} \times 100 \quad [2]$$

2.8 Cargo loading

The cargo loading (CL) of ironized and multivitamin-loaded liposomes was determined by measuring the encapsulated vitamins and iron present in the concentrated liposomes separated by centrifugation. For vitamin C and E, the cargo contents were measured by UV/Vis Spectrophotometry at wavelengths of 265 and 295 nm, respectively. Iron content in the liposomes was quantified by using ICP-AES. The total mass of the liposomes was simply measured by measuring the collector before and after the

experiment. The EE values were applied to subtract the un-encapsulated cargo from the total mass of the liposomes. Finally, the CL (%) was measured using equation 3:

$$CL (\%) = \frac{\text{Weight of cargo in liposomes}}{\text{Total weight of liposomes}} \times 100 \quad [3]$$

2.9 Statistical Analysis

The values of liposome size, EE%, and CL% were reported as a mean \pm standard error for different samples. Analysis of variance (ANOVA) was used to study the significant differences between means at a significance level of $p < 0.05$.

2.10 Simulation of the Mixing Process

Solidworks® software was used to create the three-dimensional geometry of the educator-nozzle system. The finite volume method (FVM) was applied to simulate the mixing of the two fluid streams (i.e. CO₂ and the hydrophilic cargo solution) inside the educator using the flow simulation module of the software. Here, the effect of the hydrophilic cargo introduction stream on the flow trajectories, streamlines, and velocity distributions of the fluids in the educator were investigated. Tetrahedral meshes were applied for each case, with and without streams and mesh-independent study was done to optimize the size of the cell. The number of tetrahedral cells were 72,470 and 60,349 when the educator with and without the cargo introduction stream was modelled, respectively; and 3D Navier-Stokes equations, which consist of conservation of mass, momentum, and energy equations, were solved. The flow regime was assumed to be turbulent, and for the turbulent kinetic energy and dissipation rate, the k- ϵ model was applied. Other assumptions included the steady-state condition for the mixing process

and no-slip boundary condition for the walls of the educator. For the CO₂ inlet, the pressure of 12, 15, and 18 MPa and temperature of 60 °C were used as the boundary condition. The effects of the phospholipid and vitamin E, which was dissolved in SC-CO₂, on the velocity and streamline of the fluid were assumed to be negligible. For the second inlet, where the hydrophilic cargo solution was pulled into the educator due to vacuum, the atmospheric pressure and temperature of 90 °C were used.

3. Results and Discussions

The confocal laser scanning microscopy (CLSM) images of the FITC-encapsulated liposomes made by using lecithin with two PC concentrations of 39% and 13% were shown in **Figure 3 (a-b, S1)** and **(c-d)**, respectively. The SC-CO₂ pre-expansion pressure and temperature were 18 MPa and 60°C, for both of the coating materials. In addition to CLSM images, the SEM images of the liposomes made from 39% and 13% PC were shown in **Figure 4 (a)** and **(b-c)**, respectively. It was observed that when lecithin with 39% PC was used, ULV and MLV liposomes were created, whereas lecithin with 13% PC change the structure of the liposomes to MVV.

In addition to liposome type, structure, and morphology, the repulsive force of both colloidal systems was measured to obtain the surface charge of the liposomes, which plays a significant role on the stability of the system. Zeta potential values, which represent the surface charge of the liposomes, are demonstrated in **Figure 5 (a)** and **(b)** for the liposomes made using 39% and 13% PC, respectively; for three different expansion pressures of 12, 15, and 18 MPa. It was observed that change in expansion pressure did not cause any significant difference in the liposomal surface charge. The

average zeta potential values were -29 mV and -40 mV for the liposomes made using coating material with PC concentrations of 13% and 39%, respectively. The higher surface charge for the 39% PC containing liposome could be attributed towards the higher density of phospholipid head-groups in it than its 13% counterpart. The colloidal system would be stable as long as the absolute value of zeta potential is above 30 mV.³³ Therefore, the liposomes made with 39% PC were in the stable range and the ones made with 13% PC were at the border.

Based on our microscopic images (**Figure 3** and **4**), it was found that most of the liposomes made with 13% PC were MVV; whereas, the liposomes made using lecithin with 39% PC content were MLV. Additionally, it was observed that when the lecithin with 39% PC was mixed with the lipophilic material, i.e. cholesterol, or vitamin E, no liposomes were formed. This could be attributed to different reasons: First, although Performix™E soy lecithin has higher concentration of phosphatidylcholine (PC), it includes less concentration of phosphatidylinositol (PI), which can play a significant role on the interaction with both of the hydrophilic and hydrophobic cargos. PI is a unique phospholipid with negative charge and five hydroxyl groups and its higher concentration in Performix™E soy lecithin could help to provide a stronger affinity to hydrophilic cargos, i.e. vitamin C and positively charged Iron sulfate compared to SOLEC FP 40. Additionally, PI possesses highly non-polar fatty acid chain that could provide a lipophilic microenvironment for vitamin E and cholesterol to be attached on or in the bilayer.^{34, 35} PI could also change the dynamic and structure of the bilayer and enhance its fluidity.³⁶ Second, in the Vent-RESS system, during expansion stage, the velocity of the PC containing SC-CO₂ gets significantly increased at the nozzle and a vacuum was created

due to the Bernoulli effect. The vacuum at vena contracta facilitated the suction of aqueous cargo inside the eductor, where it gets fragmented into miniscule droplets due to high shear force exerted by the released CO₂ stream and the nucleating PC molecules. During this stage the liposome formation was dictated by two factors, how much PC was phase separating from the CO₂ stream and how quickly they were coating around water droplets. In our previous work we measured the solubility of both the lecithins used in this work.^{2, 22} It was observed that SOLEC FP 40 with 39% PC had higher solubility in SC-CO₂ than Performix™E soy lecithin with 13% PC. In this condition, for the 13% PC containing lecithin, due to lower solubility, it had less amount of PC in the expansion stage, which coated around water droplet as soon as possible to attain stability. However, the 39% PC containing lecithin had higher solubility, which resulted in having more nucleation sites in the mixing part of the nozzle and self-stability by aggregation through micelle formation. Third, vitamin E might decrease the fluidity of the hydrocarbon domain of PC at temperature below its melting point. In 39% PC containing lecithin, due to higher PC content the interaction between vitamin E and PC further restricted motional freedom of the components in the mixture and thus inhibited liposome formation.³⁷ Therefore, the lecithin with 13% PC was found to be more in accordance with the goals of this study, mainly because it could form liposomes when two hydrophilic and one hydrophobic cargos were involved in the process. Additionally, this type of lecithin formed MVV liposomes, which are good candidates for encapsulating hydrophilic and entrapping lipophilic cargos^{3, 38}. Thus, only the lecithin with 13% PC was used for microencapsulation of our current cargo, i.e. iron sulfate, and vitamins C, and E and characterization of the process and products.

As described earlier, the SC-CO₂ process was coupled with vacuum-driven cargo loading to mix the hydrophilic and hydrophobic materials in an educator-nozzle system and produce liposomes with a high production rate. Therefore, there was no need to use an external pump to inject the cargo solution into the system. **Figure 6** shows the cargo solution flow rate pulled into the system at different pressures. It was found that the cargo flow rate increased by 25% when the pressure increased from 12 to 18 MPa due to the fact that higher pressure was converted to the higher velocity after the nozzle which resulted in creation of higher vacuum in the eductor (Bernoulli's principle). The operating conditions, pressure and temperature, plays a significant role on solubility of the lipophilic part of the liposome in the SC-CO₂, atomizing the hydrophilic solution, mixing efficiency between two fluids. All of these factors can affect the size, uniformity, and encapsulation efficiency of the cargos into the liposomes. **Figure 7 (a)** and **(b)** represent the effect of pressure on average size and size distribution of the resulting liposomes, respectively. **Figure 7 (a)** shows unimodal distributions of the liposomes made at three different pressures of 12, 15, and 18 MPa. **Figure 7 (b)** demonstrates that the average diameter of the liposomes increased from 578 to 698 nm. That is because at higher pressure, the solubility of the lipophilic compounds in the SC-CO₂ increased, therefore causing a greater portion of the lipophilic cargo and coating materials to precipitate and form larger liposomes. However, when the pressure increased from 15 MPa to 18 MPa, the average diameter of the liposomes reduced slightly by 3%. Here, although the solvating power of SC-CO₂ increased at higher pressure, the velocity gradient between two fluids increased as well. This caused higher shear force at the fluid/fluid interface which led to breaking the water-phase into smaller droplets, which were coated with the lipophilic compounds

in a more enhanced mixing and form smaller liposomes.^{39, 40} Tsai and Rizvi observed the same correlation between the pressure of SC-CO₂ and average size of the resulting liposomes.²

Figure 8 (a) shows the encapsulation efficiency (EE) of two hydrophilic cargos: vitamin C and iron sulfate, and one hydrophobic cargo: vitamins D, in the liposomes created using three different pressures of 12, 15, and 18 MPa. The results show that the EE increased when higher pressure was used for all of the cargos. That was expected because the density of SC-CO₂ was higher at the pressure of 18 MPa, which resulted in higher solubility of the coating material in SC-CO₂.² Therefore, when the concentration of the coating materials in SC-CO₂ increased, a higher percentage of the atomized hydrophilic cargo was coated in the eductor during the depressurization of CO₂ and supersaturation of the coating materials. The solubility of vitamin E and PC reduces significantly with reduction of pressure, especially in the lower pressure of 12-15 MPa.²⁶ This is the reason poor EE was observed at lower pressure region. However, vitamin E's EE increased significantly with the increase of pressure, because vitamin E along with coating material PC demonstrates higher solubility in SC-CO₂ at higher pressure. Thus, with the increase in pressure higher amount of vitamin E got incorporated inside the coating material and thus higher EE was observed. For vitamin C and iron, encapsulation efficiency was mostly dependent on the amount of aqueous cargo that got sucked into the vacuum formed inside the educator. As presented in **Figure 6**, with increase in pressure the flow rate of aqueous cargo increases as well, and more PC is also present at higher operating pressure condition. A larger amount of aqueous cargo got coated by PC layer and consequentially higher EE was also observed.

In **Figure 8 (b)**, the cargo loading (CL) of three different micronutrients are demonstrated. For Vitamin E and C no substantial difference was observed in CL across three different pressure points. However, the CL of Iron in the liposomes enhanced by a factor of 2.3 when the pressure was increased from 12 to 18 MPa. The obtained CL values were greatly dictated by the initial cargo loading during liposome formation. Also, a reverse relation was observed between CL and EE: maximum EE was observed for vitamin E, which demonstrated the minimum CL. Yang et al. synthesized bile salt containing liposomes by using a SC-CO₂ assisted method (i.e. solution-enhanced dispersion by supercritical fluids) to enhance bioavailability and dissolution of a lipophilic hepatoprotective agent silymarin.⁴¹ To optimize the processing condition, a central composite design of response surface methodology was used. For silymarin, they obtained an EE and drug loading values of 91.4 and 4.73%, respectively. However, their work involved with a mixture of organic solvent consisting of ethanol and dichloromethane. In a similar work, Jia et al. encapsulated an active anti-cancer and anti-inflammatory phytochemical curcumin in liposomes.⁴² They synthesized liposomes by using ethanol as a solvent and SC-CO₂ as an antisolvent along with ultrasound treatment and optimized the EE and drug loading at 79.0 and 8.9%, respectively. Head-to-head comparison of EE and CL values from this work to that of other studies would be unrealistic, owing to substantial difference in processing condition which include but not limited to wide variation in operational techniques and parameters, incorporation of cosolvents, types and numbers of cargo getting encapsulated.

Beside the experimental work, the mixing of two fluids, (i.e. CO₂ and hydrophilic cargo solution) in the eductor was numerically simulated using FVM, and the results are

shown in **Figure 9**. In this figure, two configurations of the eductor (**a**) with and (**b**) without the cargo introduction tube were compared in terms of flow trajectories, streamlines, and velocity distributions. For both the cases, the mixing of the two fluids occurred due to the depressurization of CO₂, increase of its velocity while passing through the nozzle, which resulted in creation of low-pressure region after the nozzle (Bernoulli's principle) and suction of the hydrophilic cargo solution into the eductor. The results of flow trajectories (**Figure 9 (a₁)** and (**a₂)**) and streamline (**Figure 9 (b₁)** and (**b₂)**) show that the cargo introduction tube location played a significant role in localizing the hydrophilic cargo, right below where the lipophilic cargo and the phospholipid supersaturation and precipitation occurred, as opposed to the case of not using the cargo pipe where the hydrophilic cargo solution was mostly wasted by dispersing in different and unwanted directions and not mixing adequately with the carbon dioxide stream. In addition to the direction of two fluids, the magnitude of the velocity of the fluids were calculated. While the velocity of the flow in the main CO₂ direction was the same for both cases of with and without the pipe, the velocity of the hydrophilic cargo was decreased by a factor of 1.7 when the hydrophilic cargo solution pipe was used. That was expected due to the increase of the hydrodynamic resistance, originating from using the pipe with smaller diameter and longer length compared to the case without the pipe. The decrease of the hydrophilic cargo solution volume into the eductor also had a significant effect on the stability of the liposome since reduced amount of ferrous sulfate in the eductor resulted in lower concentration of the uncoated ferrous sulfate molecules in the final product, which were subsequently separated from the coated ones in this study by using cationic exchange resins.

Additionally, the effect of pressure on the streamline and velocity distribution of the fluids in the eductor-nozzle system with the cargo introduction tube was investigated (**Figure 10**). The increase of pressure from 12 to 18 MPa, had negligible effects on the streamline of the fluids. This indicates that the difference between the EE at different pressures of 12, 15, and 18 MPa was mainly due to the significant difference in the solvating power of the SC-CO₂, and the mixing condition was not significantly altered by changing the pressure from 12 to 18 MPa.

Conclusions:

Ironized multivitamin-loaded liposomes were produced using SC-CO₂ in the Vent-RESS system without the aid of any organic solvent or external energy to pump the hydrophilic cargo and mix it with the coating material. The effect of two different coating materials on the structure and surface charge of the liposomes were studied, and one of them was selected to generate ironized multivitamin-loaded liposomes due to a better interaction with the two hydrophilic cargos (i.e. iron sulfate and vitamin C) in the core and one hydrophobic cargo (i.e. vitamin E) in the shell compartments. The effect of pressure on the size, size distribution, and encapsulation efficiency of the cargo were studied. It was found that when the pressure increased from 12 to 15 MPa, the average size increased by a factor of 1.2. Then, there was no a significant difference between the average size of the liposomes when the pressure was raised to 18 MPa. Additionally, the EE of all of the cargos was improved when the pressure increased from 12 to 18 MPa due to higher solvating power of the SC-CO₂ and enhanced mixing between the atomized hydrophilic and lipophilic phases. Additionally, the mixing process of the two fluids was numerically simulated using Finite Volume Method (FVM) to understand the effect of the

cargo introduction geometry on guiding the hydrophilic cargo in the educator right below where supersaturation and precipitation of lipophilic cargo carried by supercritical fluid occurred. The current ironized multivitamin loaded liposomes should be considered for use in fortification of food and pharmaceutical products because no toxic, organic solvents are used in this proposed, novel technology, which is very amenable to scale-up for commercial utility.

Acknowledgements

The authors would like to thank US Agricultural Department National Institute of Food and Agriculture (USDA-NIFA), grant: 2017-67017-26474 for financially supporting this project. The Cornell University Biotechnology Resource Center (BRC), grant NIH S10RR025502 is also acknowledged for their assistance with the confocal microscopy. We also wish to thank Andrew Melnychenko for his help in this work.

Conflicts of interest

There are no conflicts to declare.

References:

1. W.-C. Tsai and S. S. H. Rizvi, *Trends in Food Science & Technology*, 2016, **55**, 61-71.
2. W.-C. Tsai and S. S. H. Rizvi, *Food Research International*, 2017, **96**, 94-102.
3. W.-C. Tsai and S. S. H. Rizvi, *Food Research International*, 2017, **99**, 256-262.
4. N. Grimaldi, F. Andrade, N. Segovia, L. Ferrer-Tasies, S. Sala, J. Veciana and N. Ventosa, *Chemical Society Reviews*, 2016, **45**, 6520-6545.
5. H. Xing, K. Hwang and Y. Lu, *Theranostics*, 2016, **6**, 1336-1352.
6. T. M. Taylor, J. Weiss, P. M. Davidson and B. D. Bruce, *Critical Reviews in Food Science and Nutrition*, 2005, **45**, 587-605.
7. D. D. Lasic, *Trends in Biotechnology*, 1998, **16**, 307-321.
8. A. Abbaspourrad, S. S. Datta and D. A. Weitz, *Langmuir*, 2013, **29**, 12697-12702.

9. C. Martino, S.-H. Kim, L. Horsfall, A. Abbaspourrad, S. J. Rosser, J. Cooper and D. A. Weitz, *Angewandte Chemie International Edition*, 2012, **51**, 6416-6420.
10. C. Decker, H. Schubert, S. May and A. Fahr, *Journal of Controlled Release*, 2013, **166**, 277-285.
11. Y. Takechi-Haraya, K. Sakai-Kato, Y. Abe, T. Kawanishi, H. Okuda and Y. Goda, *Langmuir*, 2016, **32**, 6074-6082.
12. K. Tai, X. He, X. Yuan, K. Meng, Y. Gao and F. Yuan, *Colloids and Surfaces A: Physicochemical and Engineering Aspects*, 2017, **518**, 218-231.
13. S. Alavi, A. Haeri and S. Dadashzadeh, *Carbohydrate Polymers*, 2017, **157**, 991-1012.
14. M. Frenzel and A. Steffen-Heins, *Food Chemistry*, 2015, **173**, 1090-1099.
15. B. C. Keller, *Trends in Food Science & Technology*, 2001, **12**, 25-31.
16. T. Nii and F. Ishii, *International Journal of Pharmaceutics*, 2005, **298**, 198-205.
17. D. Deamer and A. D. Bangham, *Biochimica et Biophysica Acta (BBA) - Biomembranes*, 1976, **443**, 629-634.
18. J. M. DeSimone, *Science*, 2002, **297**, 799-803.
19. T. Imura, T. Gotoh, K. Otake, S. Yoda, Y. Takebayashi, S. Yokoyama, H. Takebayashi, H. Sakai, M. Yuasa and M. Abe, *Langmuir*, 2003, **19**, 2021-2025.
20. A. Montes, M. D. Gordillo, C. Pereyra and E. J. M. d. I. Ossa, *Mass Transfer: Advanced Aspects*, 2011, 461-480.
21. K. Otake, T. Shimomura, T. Goto, T. Imura, T. Furuya, S. Yoda, Y. Takebayashi, H. Sakai and M. Abe, *Langmuir*, 2006, **22**, 4054-4059.
22. F. Sharifi, R. Zhou, C. Lim, A. Jash, A. Abbaspourrad and S. S. H. Rizvi, *Journal of CO2 Utilization*, 2019, **29**, 163-171.
23. S. Yokoyama, T. Takeda and M. Abe, *Colloids and Surfaces B: Biointerfaces*, 2003, **27**, 181-187.
24. X. Liang, G. Mao and K. Y. S. Ng, *Journal of Colloid and Interface Science*, 2004, **278**, 53-62.
25. K. Nakano, Y. Tozuka, H. Yamamoto, Y. Kawashima and H. Takeuchi, *International Journal of Pharmaceutics*, 2008, **355**, 203-209.
26. M. Johannsen and G. Brunner, *Journal of Chemical & Engineering Data*, 1997, **42**, 106-111.
27. Á. M. Salima Varona, María José Cocero, 2016, ch. 2.
28. S. R. R. Á Martín, A Navarrete, *Journal*, 2013.
29. M. E. Wagner and S. S. H. Rizvi, *Journal of Liposome Research*, 2015, **25**, 334-346.
30. P. T. Ingvarsson, M. Yang, H. M. Nielsen, J. Rantanen and C. Foged, *Expert Opinion on Drug Delivery*, 2011, **8**, 375-388.
31. R. R. C. New, *Liposomes: A practical approach*, Oxford University Press (Chapter 3), New York, 1990.
32. M. E. Wagner, K. A. Spoth, L. F. Kourkoutis and S. S. H. Rizvi, *Journal of Liposome Research*, 2016, **26**, 261-268.
33. B. Heurtault, P. Saulnier, B. Pech, J.-E. Proust and J.-P. Benoit, *Biomaterials*, 2003, **24**, 4283-4300.
34. H. Minami, M. Iwahashi and T. Inoue, in *Studies in Surface Science and Catalysis*, eds. Y. Iwasawa, N. Oyama and H. Kunieda, Elsevier, 2001, vol. 132, pp. 615-618.

35. G. F. Combs, in *The Vitamins (Fourth Edition)*, ed. G. F. Combs, Academic Press, San Diego, 2012, DOI: <https://doi.org/10.1016/B978-0-12-381980-2.00018-9>, pp. 395-433.
36. A. Peng, D. S. Pisal, A. Doty and S. V. Balu-Iyer, *Chemistry and Physics of Lipids*, 2012, **165**, 15-22.
37. X. Wang and P. J. Quinn, *Progress in Lipid Research*, 1999, **38**, 309-336.
38. C. Anandharamakrishnan, in *Techniques for Nanoencapsulation of Food Ingredients*, Springer New York, New York, NY, 2014, DOI: 10.1007/978-1-4614-9387-7_3, pp. 17-28.
39. S. Li and Y. Zhao, *Int J Nanomedicine*, 2017, **12**, 3485-3494.
40. J. J. Harrison, C. Lee, T. Lenzer and K. Oum, *Green Chemistry*, 2007, **9**, 351-356.
41. G. Yang, Y. Zhao, Y. Zhang, B. Dang, Y. Liu and N. Feng, *Int J Nanomedicine*, 2015, **10**, 6633-6644.
42. J. Jia, N. Song, Y. Gai, L. Zhang and Y. Zhao, *The Journal of Supercritical Fluids*, 2016, **113**, 150-157.

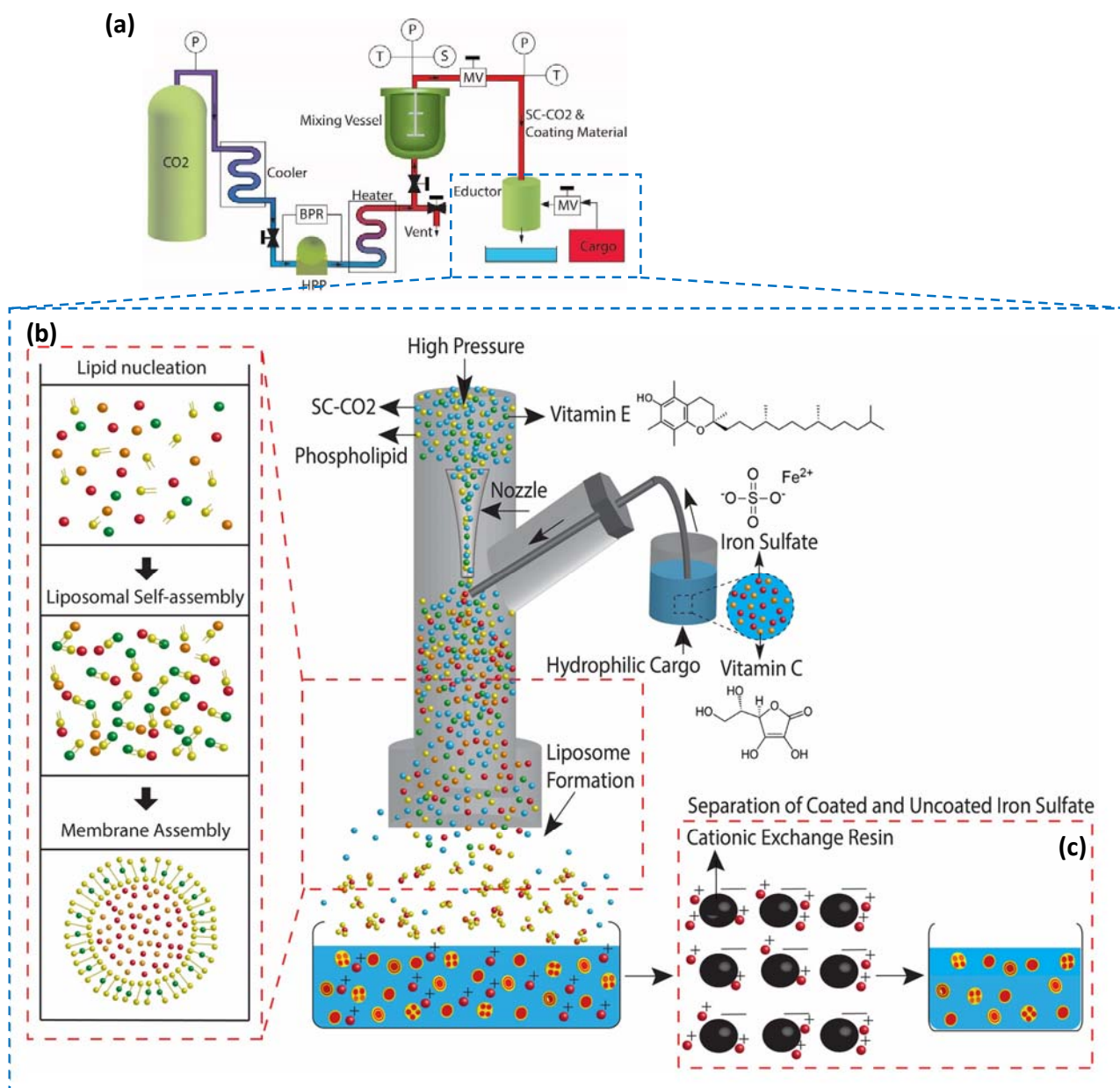
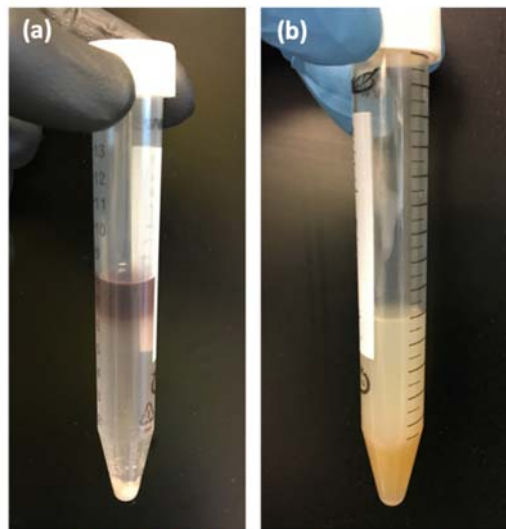


Figure 1 (a) Schematic representation of the Vent-RESS system. The following terms are used: BPR: back pressure regulator, HPP: high-pressure pump, MV: metering valve, S: safety valve, P: pressure indicators, T: temperature indicators. (b) Enlarged view of the eductor nozzle, with a step-by-step schematic of liposome formation within the eductor. (c) Using the cationic exchange resins for separation of the coated and uncoated iron sulfate, which substantially helped to increase the stability of the liposomes and prevent their rupture.



After 10 min **After 10 days**

Figure 2 (a) Unstable liposomes: Cationic exchange ion resins were not used. Color change and liposome rupture occurred right after liposome production due to the oxidation of uncoated iron sulfate. Clumps of lecithin were observed at the bottom of the centrifuge tube. **(b)** Stable liposomes: Color change was not observed, and the liposomes were not ruptured. Additionally, unlike using the ion exchange column, the concentration of liposomes was not reduced.

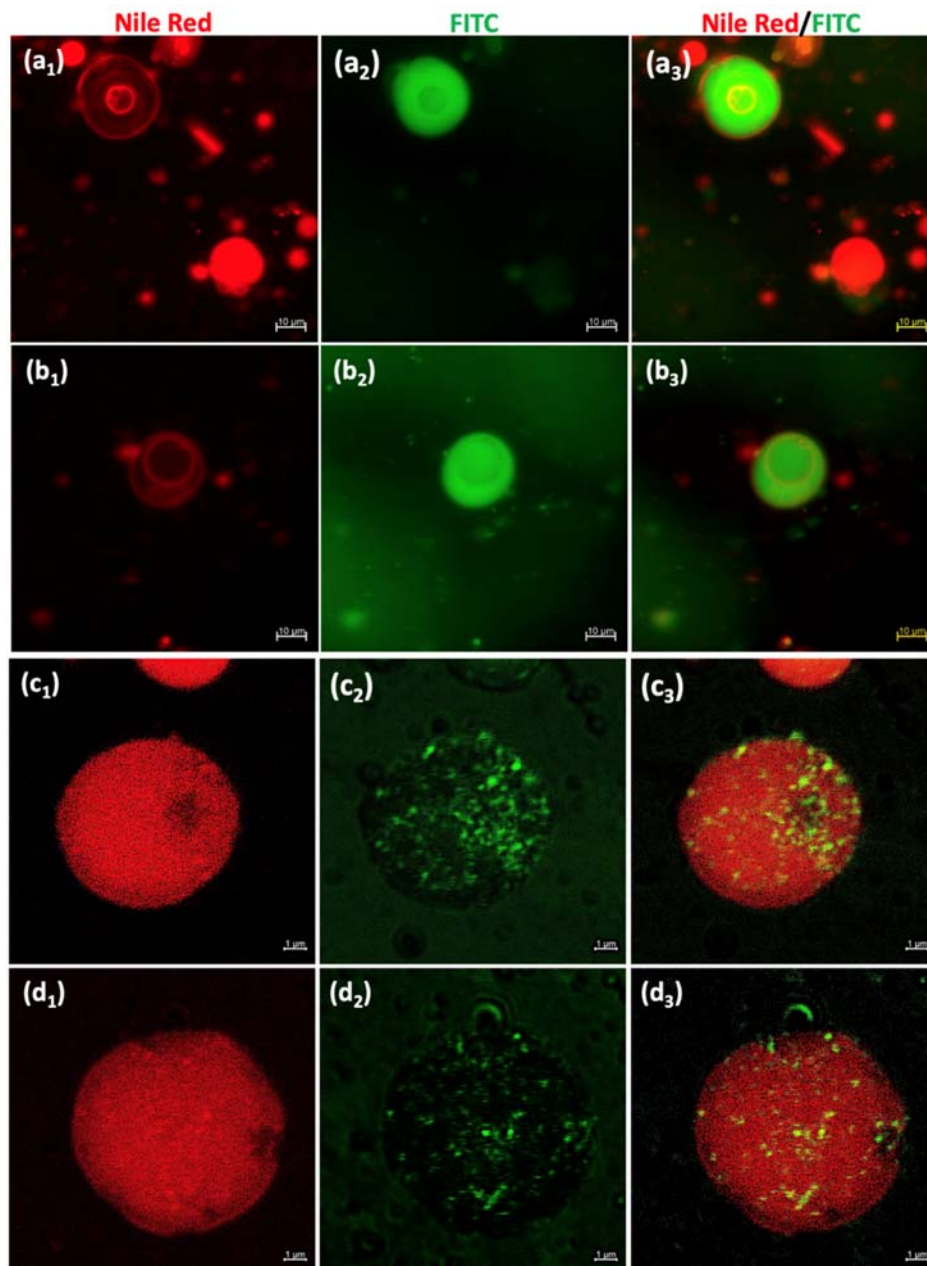


Figure 3 CLSM images of the liposomes produced at 18 MPa and 60 °C using **(a-b)** 39% PC and **(c-d)** 13% PC.

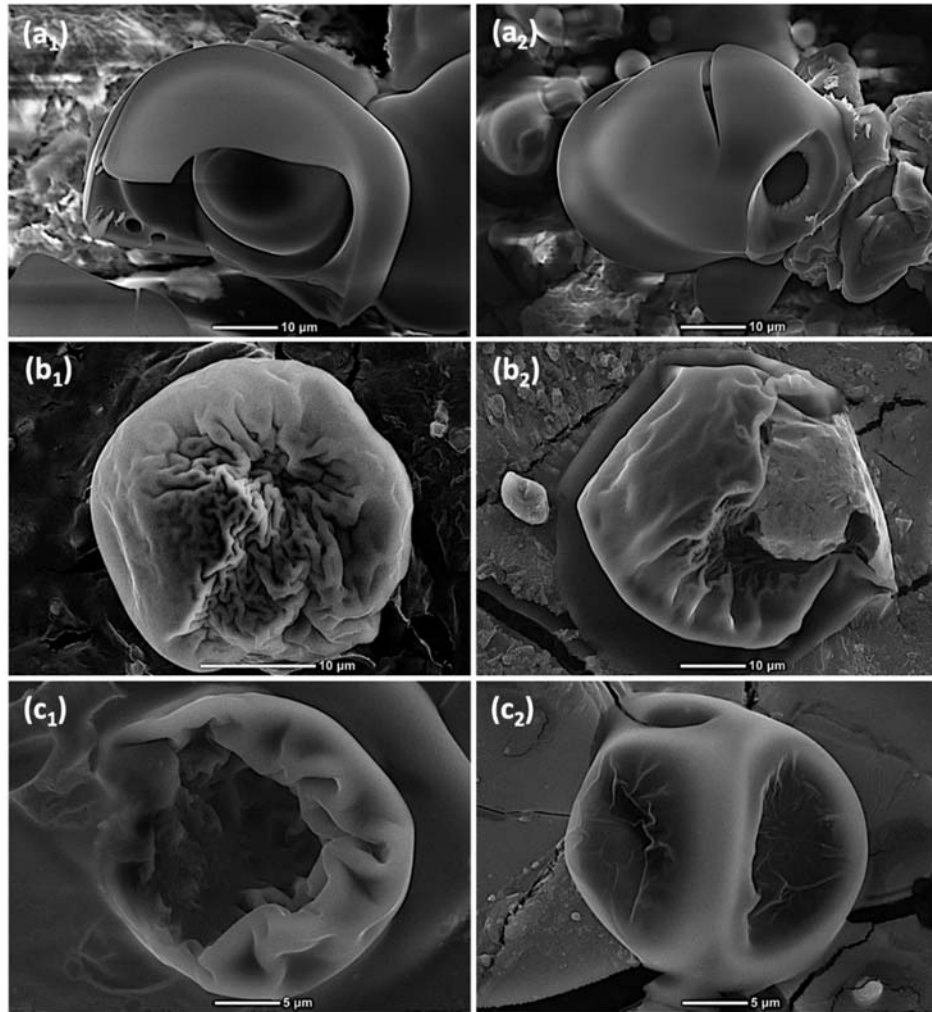


Figure 4 SEM images of the liposomes produced at 18 MPa and 60 °C using **(a)** 39% PC and **(b-c)** 13% PC.

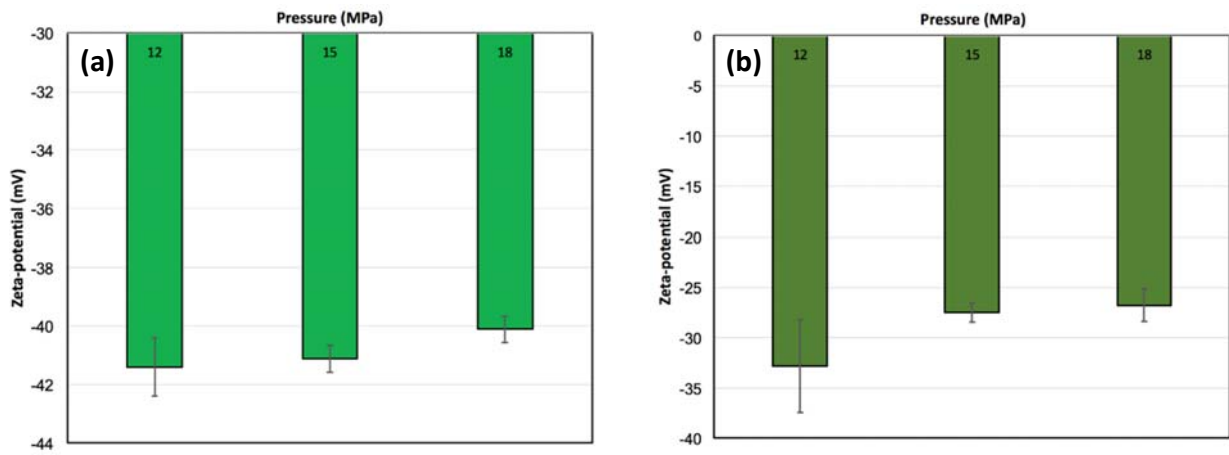


Figure 5 Zeta potential of the liposomes made with **(a)** 39% PC and **(b)** 13% PC at three different pressures of 12, 15, 18 MPa.

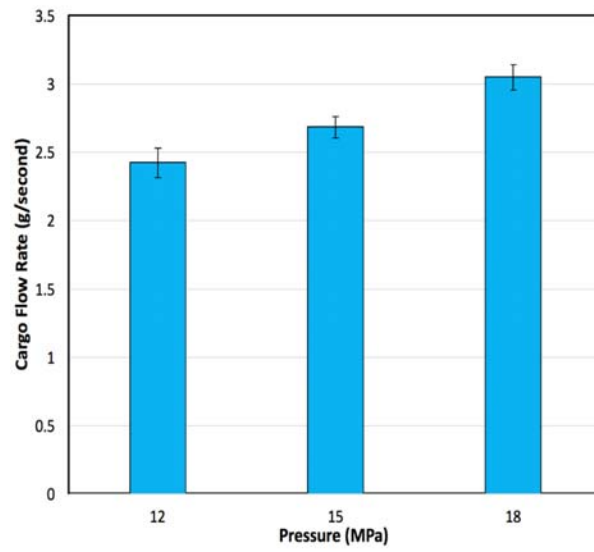


Figure 6 Effect of pressure on the hydrophilic cargo solution flow rate pulled into the eductor

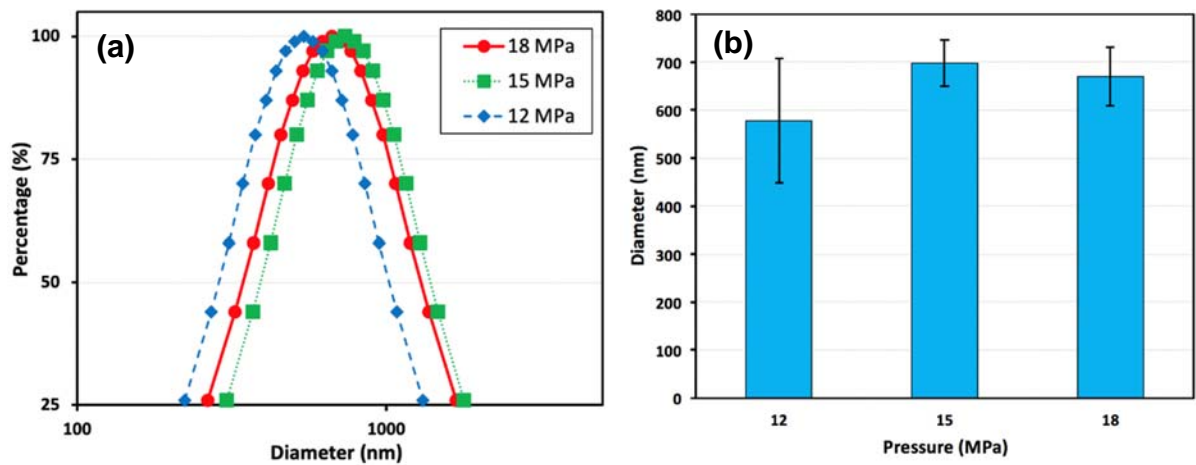


Figure 7 (a) Size distribution and **(b)** average size of the liposomes made at pressures of 12, 15, and 18 MPa.

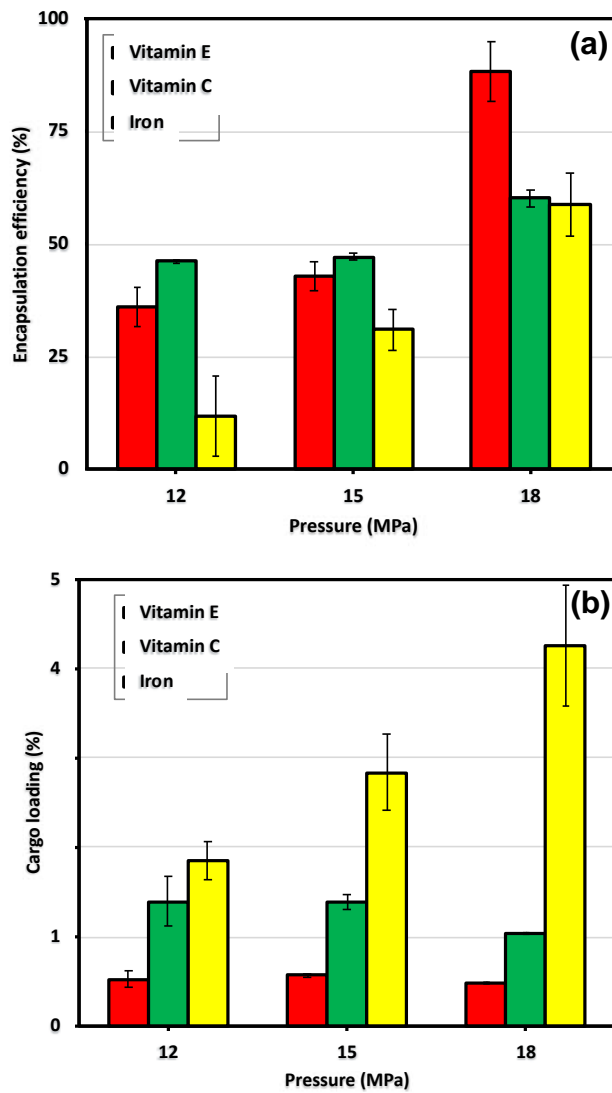


Figure 8. (a)The encapsulation efficiency and **(b)** Cargo loading for iron, vitamin C, and E in liposomes formed at three pressures of 12, 15, and 18 MPa.

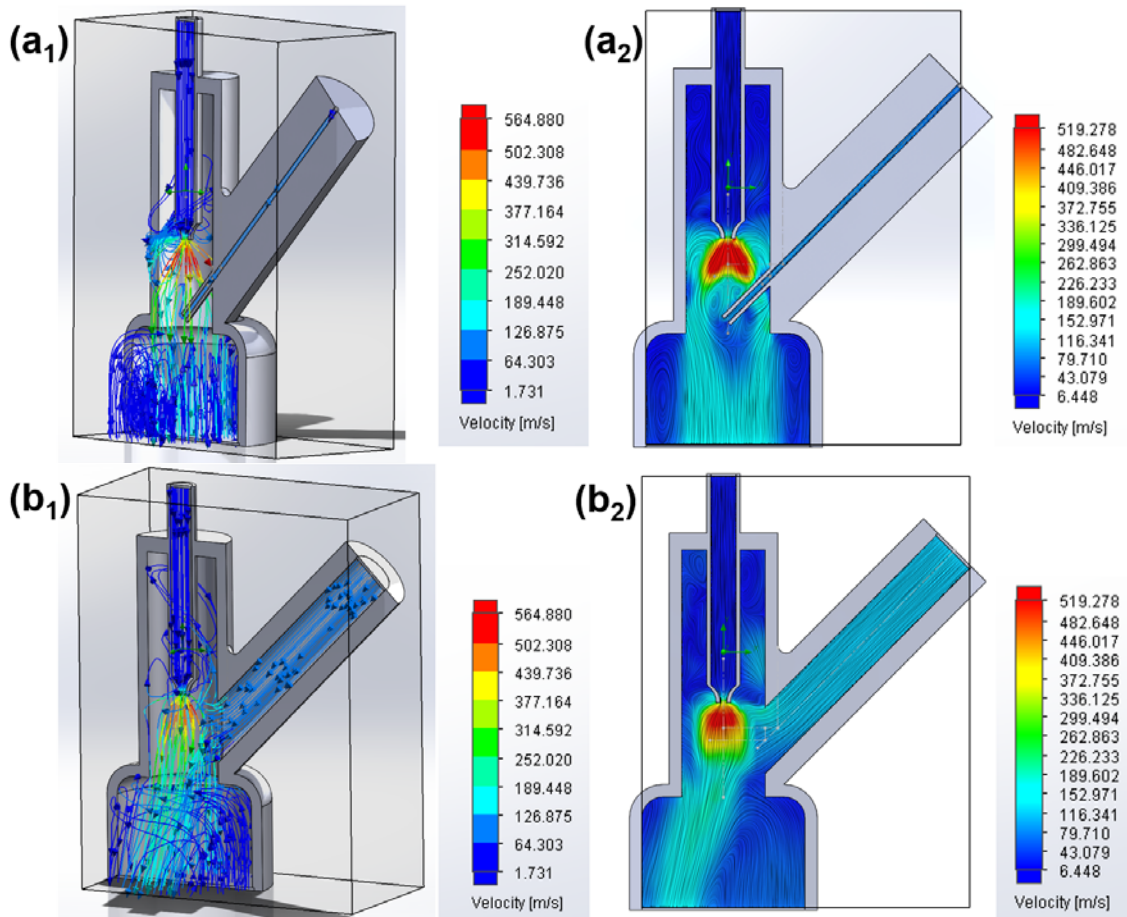


Figure 9. Comparison between two configurations in the eductor: **(a₁ - a₂)** with and **(b₁ - b₂)** without a cargo introduction pipe. **(a₁ and b₁)** Flow trajectories and **(a₂ and b₂)** streamlines and velocity distributions of the fluids in the eductor-nozzle system. For both conditions, the pressure and temperature of SC-CO₂ were 18 MPa and 60 °C, respectively.

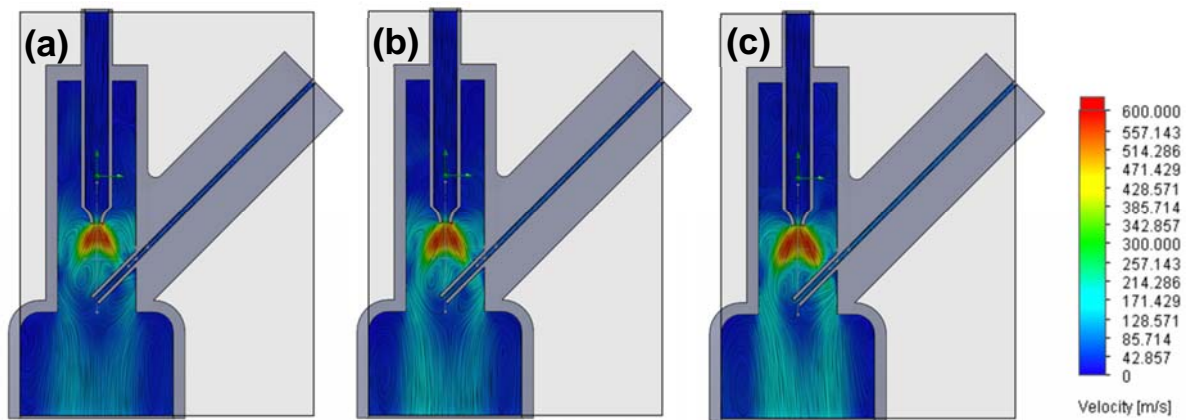


Figure 10. The streamlines and velocity distributions of the fluids in the eductor-nozzle system at **(a)** 12 MPa, **(b)** 15 MPa, and **(c)** 18 MPa. The color bar represents the fluid velocity for **(a-c)**.

Table 1. Temperature of SC-CO₂ at different locations of the system and nozzle and cargo introduction tube diameters

Nozzle diameter	1.5 mm
Cargo introduction tube diameter	1.3 mm (I.D.)
Cargo solution temperature	90 °C
Eductor nozzle temperature	90 °C
Mixing vessel temperature	60 °C